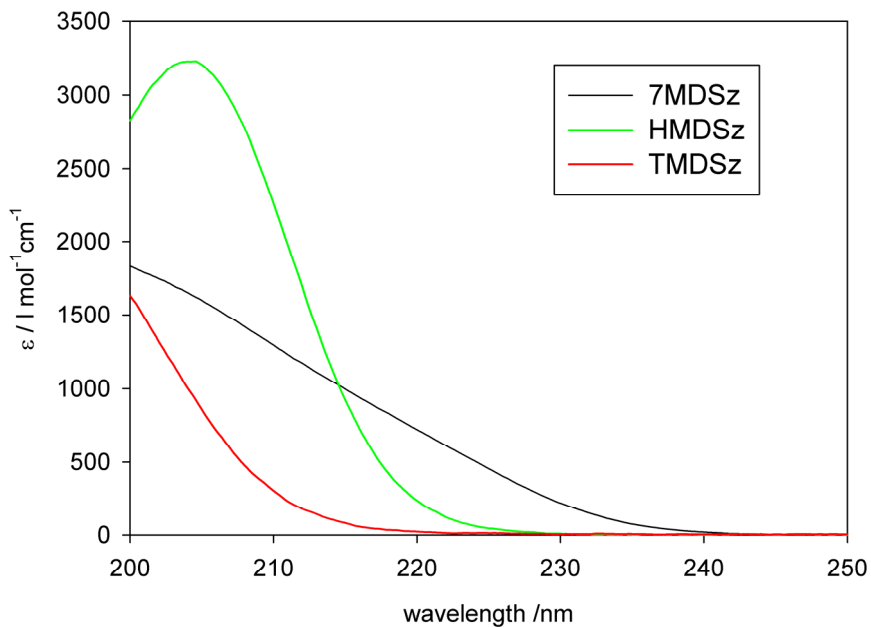
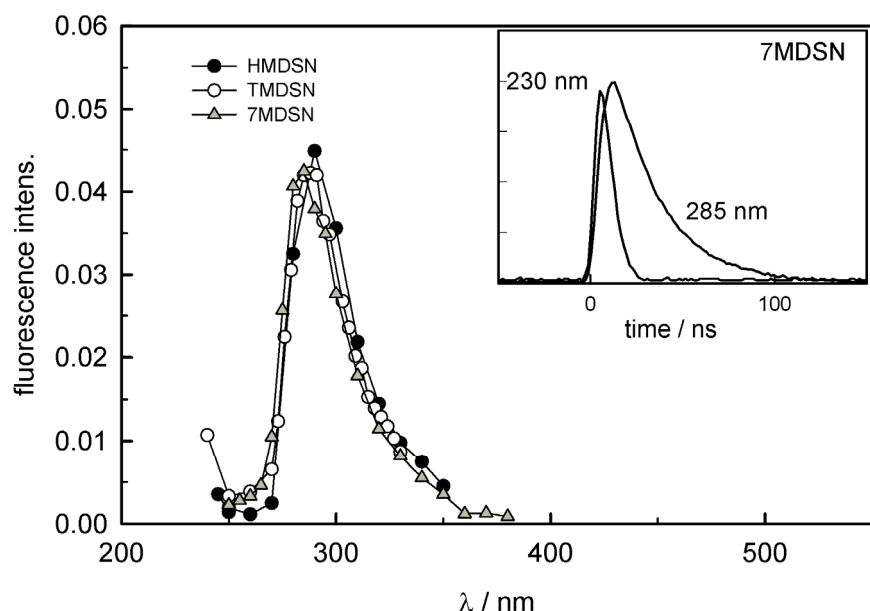


## 222 nm Photo-Induced Radical Reactions in Silazanes. A combined Laser Photolysis, EPR, GC-MS and QC Study.

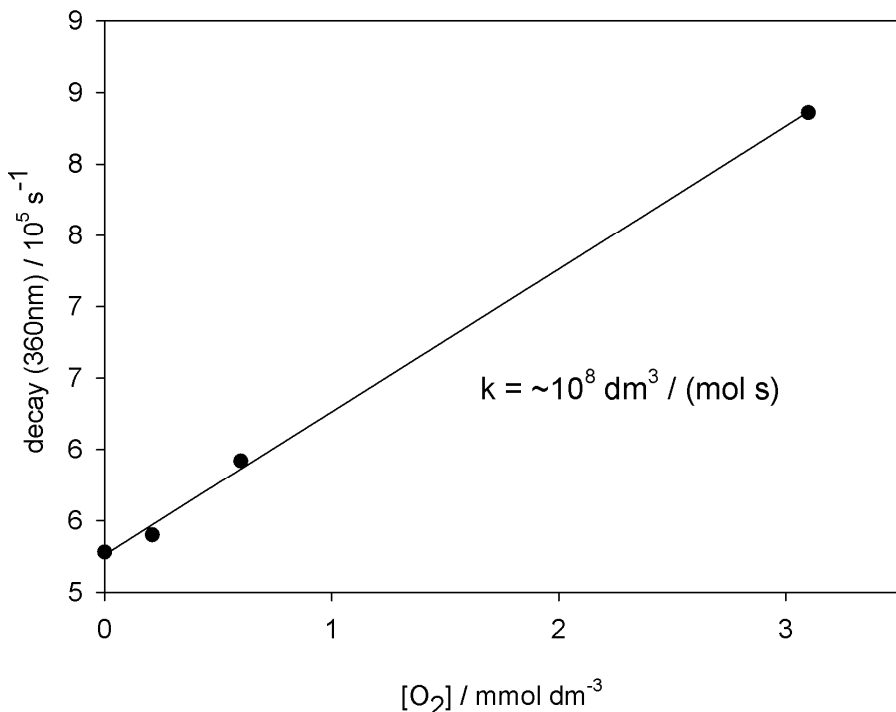
<sup>5</sup> Wolfgang Knolle,<sup>\*a</sup> Luise Wennrich,<sup>a</sup> Sergej Naumov,<sup>a</sup> Konstanze Czihal,<sup>a</sup> Lutz Prager,<sup>a</sup> Daniel Decker,<sup>b</sup> and Michael R. Buchmeiser<sup>a,c</sup>



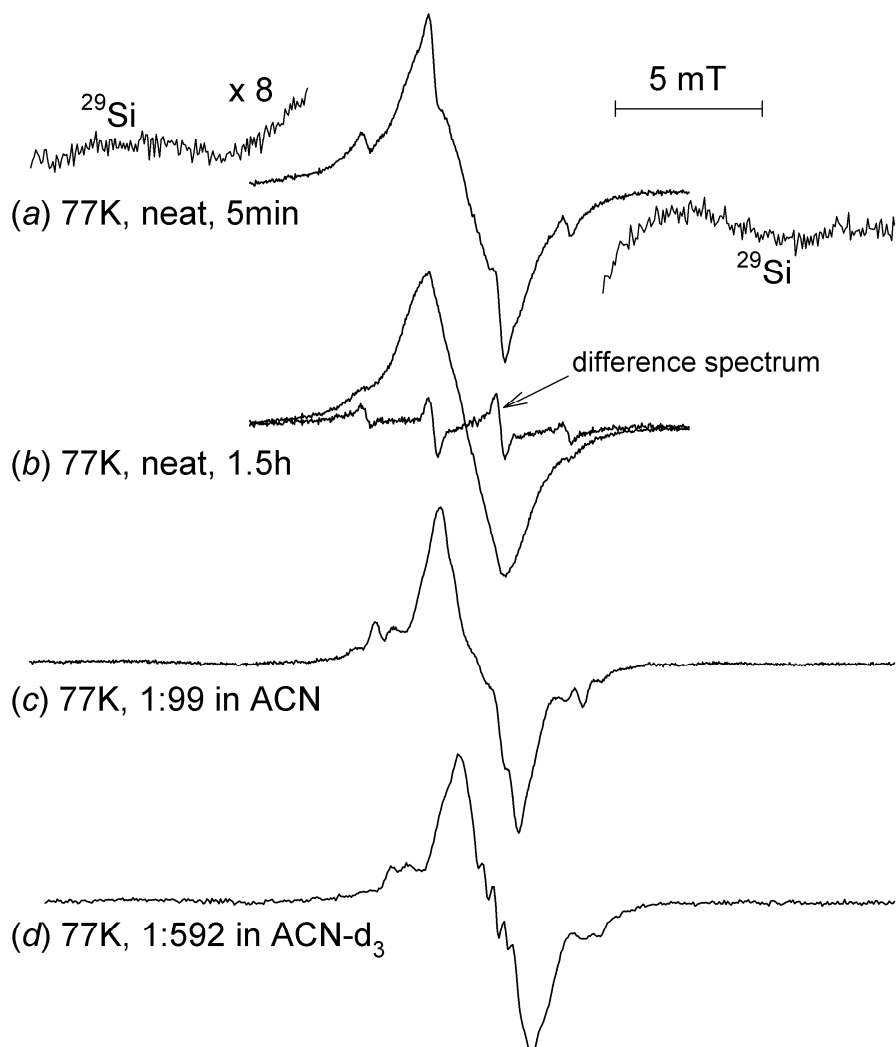
**Fig. 1S** Absorption spectra of silazanes, measured in approx.  $5 \times 10^{-3}$  M solution in acetonitrile. Molar absorption coefficients of tetra-, hexa- and heptadisilazanes at 222 nm are 16, 120 and  $615 \text{ dm}^3 \text{ mol}^{-1} \text{ cm}^{-1}$ )  
<sup>10</sup>



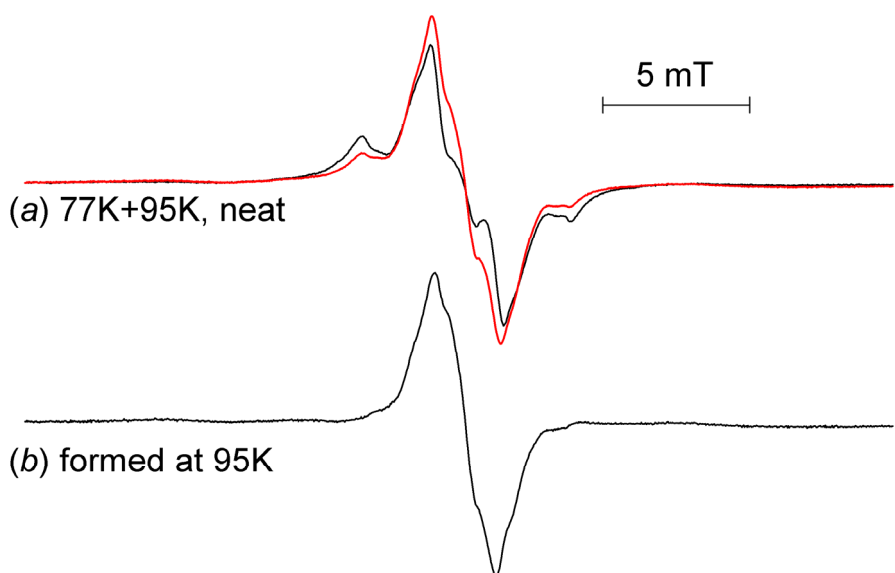
**Fig. 2S** Emission spectra observed after 222 nm laser excitation of deoxygenated solutions of TMDSz, HMDSz and 7MDSz in n-hexane. Spectra are recorded without any correction for the wavelength-dependent relative efficiency. The Inset shows time profiles at 230 and 285 nm in case of 7MDSz.



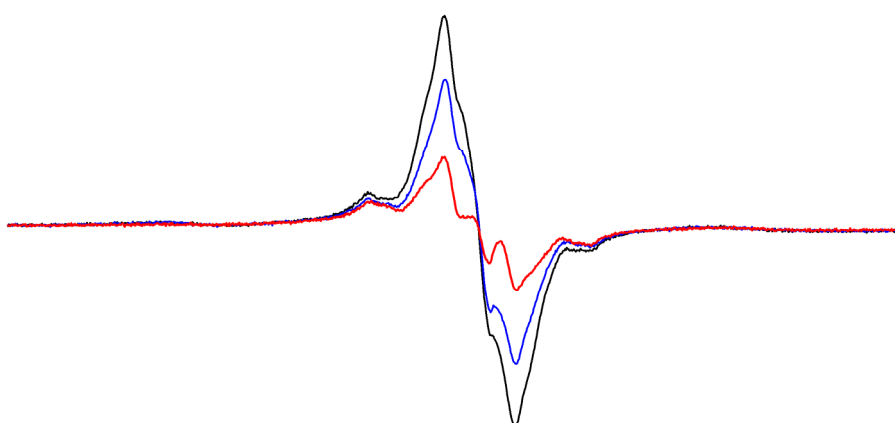
**Fig. 3S** Decay of the absorbance observed at 360 nm in 0.01 mol dm<sup>-3</sup> HMDSz / n-hexane solution after excitation with 222 nm eximer laser in dependence of the oxygen concentration. From the slope a bimolecular rate constant of  $1 \times 10^8 \text{ dm}^3 \text{ mol}^{-1} \text{ s}^{-1}$  was derived



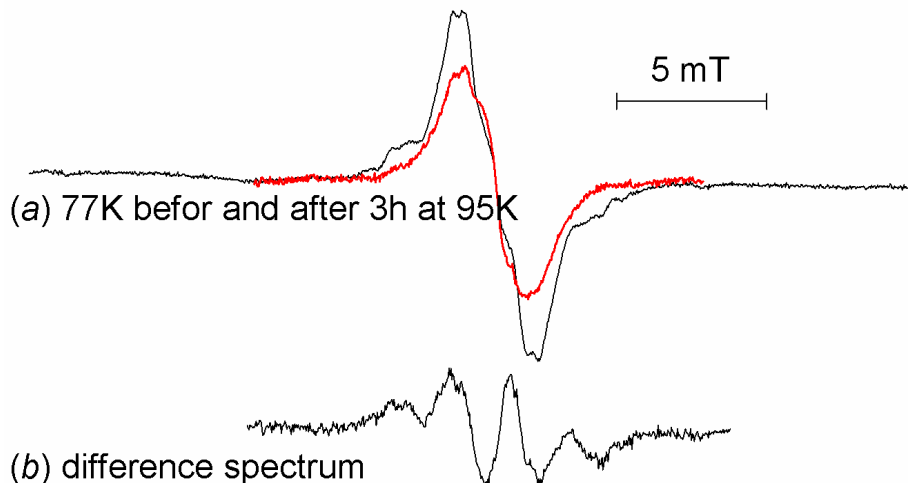
**Fig. 4S** EPR spectra observed at 77 K after 222 nm irradiation of neat TMDSz and frozen solutions of TMDSz in acetonitrile und acetonitrile-d<sub>3</sub>. The spectral changes observed (compare (a) and (b)) are mainly due to the decay of methyl radicals as evidenced by the difference spectrum in (b). Essentially the same spectra with slightly better resolution are observed in the frozen solutions (c) and (d), and the decay of methyl radicals occurs as well.



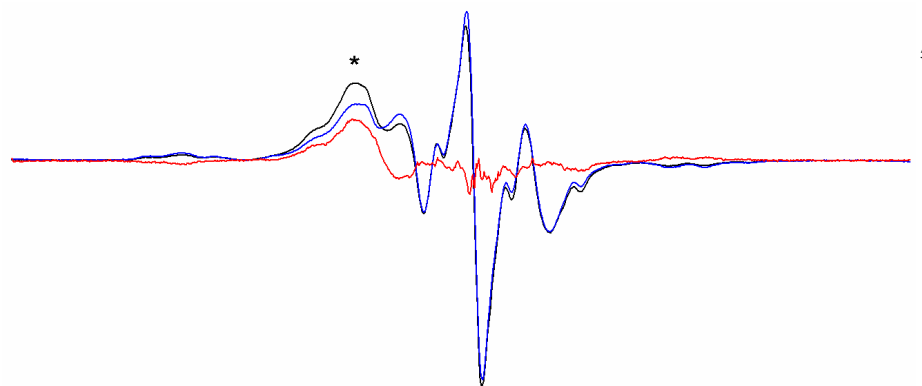
**Fig. 5S** EPR spectra observed after 222 nm irradiation of neat TMDSz at 77 K and 95 K. The decay of the methyl radicals leads to an increase of the central part of the spectrum. The spectrum formed at 95 K is given as a weighted difference in (b) and can well be attributed to silyl radicals  $^{\bullet}\text{Si}(\text{CH}_3)_2\text{-R}$ .



**Fig. 6S** EPR spectra observed after 222 nm irradiation of neat TMDSz at 100K (black), 105K (blue), and 110K (red). In this temperature interval the decay of silyl radicals occurs.



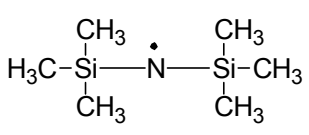
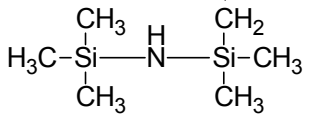
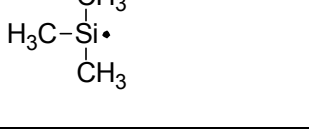
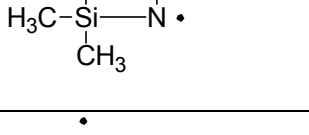
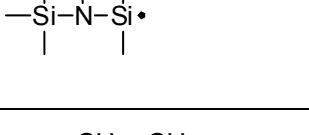
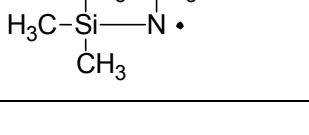
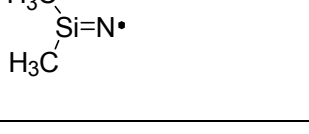
**Fig. 7S** (a) Spectra recorded at 77K after 3h (after decay of methyl radicals, black) and after 3h at 77K and 1h at 95K (decay of side bands, red) (b) difference spectrum. All spectra were taken in 1:99 ACN solution.



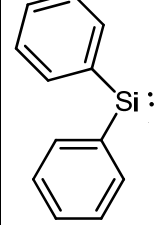
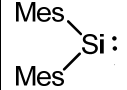
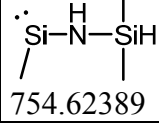
**Fig. 8S** EPR spectra observed after irradiation of HMDSz with 222 nm UV light, normalized at the central line. Irradiation time: 60s (black) and 300s (blue). Difference spectrum (red). Note the formation of a broad singlet marked with an asterisk with a g-value of ~2.022

**Table 1S** Quantum chemical calculations of heat of formation (E), hyperfine coupling constants (a) and UV transitions ( $\lambda$ ) of radicals derived from disilazanes

structure	Energy		a [G]	$\lambda$ [nm]
$\begin{array}{c} \text{CH}_3 \quad \text{H} \\   \quad   \\ \text{H}-\text{Si}-\text{N} \cdot \text{Si}-\text{H} \\   \quad   \\ \text{CH}_3 \quad \text{CH}_3 \end{array}$	755.314962	Si N $\text{H}_\text{N}$ H $\text{CH}_3$	178(26;26;52) 4.3 (-2,-2,4.5) -3.5 33 5.7 (3H)	339 (0.0078) 311 (0.0316) <b>294 (0.0919)</b> 285 (0.0139)
$\begin{array}{c} \text{CH}_3 \quad \text{H} \\   \quad   \\ \text{H}-\text{Si}-\text{N} \cdot \\   \quad   \\ \text{CH}_3 \quad \text{CH}_3 \end{array}$	425.24052	Si N $\text{H}_\text{N}$ H $\text{CH}_3$	12 12 (-12,-12, 24.5) 19.8 1.5 1.8 (6H)	<b>306 (0.0352)</b> 245 (0.0143)
$\begin{array}{c} \text{CH}_3 \\   \\ \text{H}-\text{Si} \cdot \\   \\ \text{CH}_3 \end{array}$	369.88486	Si N $\text{H}_\text{N}$ H $\text{CH}_3$	147( 25,25,50) - - 17.2 7.42 (6H)	289 (0.0277) <b>274 (0.0466)</b> <b>245 (0.0515)</b>
$\begin{array}{c} \text{CH}_3 \quad \text{H} \\   \quad   \\ \cdot \text{Si}-\text{NH} \\   \\ \text{CH}_3 \end{array}$	425.26851	Si N $\text{H}_\text{N}$ H $\text{CH}_3$	147.11 2.07 3.6 (2H) - 5.26 (6H)	344 (0.0072) 302 (0.0337) 300 (0.0699) <b>275 (0.1052)</b> <b>262 (0.1134)</b> 246 (0.0188)
$\begin{array}{c} \text{CH}_3 \quad \text{H} \quad \text{CH}_3 \\   \quad   \quad   \\ \text{H}-\text{Si}-\text{N} \cdot \text{Si}^\bullet \\   \quad   \quad   \\ \text{CH}_3 \quad \text{CH}_3 \quad \text{CH}_3 \end{array}$	794.637957	Si N $\text{H}_\text{N}$ H $\text{CH}_3$	158 (-23.7, -23.7, 47) 3.49 (-0.7, -0.5, 1.13) 6.4 - 6.6 (6H)	360 (0.0065) 303 (0.0072) <b>283 (0.0392)</b> <b>270 (0.0423)</b>
$\begin{array}{c} \text{CH}_3 \quad \cdot \quad \text{CH}_3 \\   \quad   \\ \text{H}-\text{Si}-\text{N} \cdot \text{Si}-\text{H} \\   \quad   \\ \text{CH}_3 \quad \text{CH}_3 \end{array}$	794.619907	Si N $\text{H}_\text{N}$ H $\text{CH}_3$	12.6 (2Si) 11.6 (-11.2,-10.8, 22) - 41.8/34.4 (38.1) < 1	
$\begin{array}{c} \text{CH}_3 \quad \text{H} \quad \text{CH}_2 \\   \quad   \quad   \\ \text{H}-\text{Si}-\text{N} \cdot \text{Si}-\text{H} \\   \quad   \quad   \\ \text{CH}_3 \quad \text{CH}_3 \quad \text{CH}_3 \end{array}$	-794.62230	Si N $\text{H}_\text{N}$ $2\text{H}_\alpha$ $\text{H}_\beta$ $\text{CH}_3$	14.2 0.4 4.5 22.1 9.8 1.2	
$\begin{array}{c} \text{CH}_3 \quad \text{H} \quad \text{CH}_3 \\   \quad   \quad   \\ \text{H}_3\text{C}-\text{Si}-\text{N} \cdot \text{Si}^\bullet \\   \quad   \quad   \\ \text{CH}_3 \quad \text{CH}_3 \quad \text{CH}_3 \end{array}$	833.96876	Si N $\text{H}_\text{N}$ H $\text{CH}_3$	159 (22;22,44) 4.49 3.11 - 5.31 (6H)	313 (0.0372) 307 (0.0433) <b>298 (0.0755)</b> 281 (0.0478) 267 (0.0372) 247 (0.0415)

	-873.27630	Si N H <sub>N</sub> H CH <sub>3</sub>	-11 (-0.6;0.2;0.4) 11.5 (-11, -11, 21) -  < 2.5 (6H)	<b>345 (0.1068)</b> 275 (0.0195) 218 (0.0301)
	-833.96875	Si N H <sub>N</sub> H CH <sub>3</sub>	-11 (-0.7;0.1;0.6) 11.5 (-11, -11, 21) -  < 2.5 (6H)	
	409.210945	Si N H <sub>N</sub> H CH <sub>3</sub>	144 (-24,-24,48) - - - 6.6 (9H)	<b>270 (0.138)</b> <b>247 (0.1394)</b>
	-464.570375	Si N H <sub>N</sub> H CH <sub>3</sub>	-11.5 11.9 -20.0 - 0.8	<b>302 (0.0298)</b> 254 (0.0092)
	-464.57589	Si N CH <sub>2</sub>	-13.4 0.2 21.3;21.7	
	-873.26544	Si N CH <sub>3</sub>	156 (-21,-21,43) 5.4 - - 5.3 (6H)	350 (0.0404) 318 (0.0386) 311 (0.0395) <b>285 (0.0574)</b> 249 (0.0217)
	-503.88609	Si N CH <sub>3</sub>	-11.4 13.7 30.8	289 (0.0086) <b>275 (0.0470)</b>
	423.989683	Si N H <sub>N</sub> H CH <sub>3</sub>	29 (-6, 3, 3) 8 (-13,-9, 22) - - 1.0(6H)	
	384.658772	Si N H <sub>N</sub> H CH <sub>3</sub>	30 7.87 (-13,-8, 22) - 23.75 1.53 (3H)	

**Table 2S** Comparison of quantum chemical calculations on UV transitions ( $\lambda/\text{nm}$ ) of silylenes with experimental data, in bold: most intensive transitions in the spectroscopically available region ( $> 230 \text{ nm}$ ). In parenthesis: oscillator strengths.

	theoretical	experimental	
 754.61284	<b>481 (0.0267)</b>	<b>465</b>	
	528 (0.0267) <b>311 (0.2412)</b> 288 (0.0397) 273 (0.0435) <b>250 (0.1388)</b>	515 <b>290</b> (very intensive)	
	561 (0.0146) 374 (0.0277) <b>301 (0.2809)</b> 238 (0.1985)	~580 (weak) 320 <b>280</b> (very intensive)	
 754.62389	<b>341 (0.0441)</b> 250 (0.0305) 230 (0.1487)		